

## Utilizing high-frequency elastic full-waveform inversion to overcome imaging challenges caused by a complex shallow overburden

P. Dubiel<sup>1</sup>, M. Faggetter<sup>1</sup>, N. Kiatjaroonlert<sup>1</sup>, M. Ledger<sup>1</sup>, S. Hollingworth<sup>1</sup>, A. Ratcliffe<sup>1</sup>, Ø. Runde<sup>2</sup>, P. Christian<sup>2</sup>, O.E. Aaker<sup>2</sup>, A. Bang<sup>2</sup>

<sup>1</sup> Viridien; <sup>2</sup> Aker BP

### Summary

---

Traditional imaging of the Frigg-Gamma structure in the Yggdrasil area of the Norwegian North Sea is compromised by the presence of large vertical columns of calcite cementation. These ‘cemented pipes’ have a highly contrasted seismic velocity regime compared with the surrounding sediments, causing strong wavefield scattering along their rugose boundary. Consequently, the Frigg-Gamma structure, which sits below these pipes, is in a seismically obscured area (SOA). We address the imaging challenges in this area caused by these, and other, complex overburden features with the use of elastic full-waveform inversion (FWI) using a shallow-water multi-component ocean bottom node data set. The superior modelling of the full wavefield through the elastic propagation in FWI creates a high-frequency velocity model (up to 64 Hz) that improves the imaging of primary data with reverse time migration (RTM). Yet, this primary-only image is still limited by the wavefield scattering caused by the cemented pipes. Our FWI Image reflectivity volume, derived directly from the elastic FWI, benefits from the full-wavefield contribution and can surpass the RTM volume, resulting in a significantly improved image of the SOA.

## Utilizing high-frequency elastic full-waveform inversion to overcome imaging challenges caused by a complex shallow overburden

### Introduction

The last decade has seen rapid development of full-waveform inversion (FWI) in the industry with the primary goal of yielding more accurate models and images of the subsurface. This has driven the development of alternative cost functions, as well as adding increasingly more accurate physics into the wavefield propagation (by accounting for anisotropy, viscosity, and elasticity). Historically, due to computing power limitations, most commercial FWI applications have relied on the acoustic wave equation. This assumption is valid for areas with low to mild impedance contrasts. However, in geological settings with strong elastic contrasts, the discrepancy between phase and amplitude in the wavefields modelled acoustically and elastically may lead to sub-optimal inversion results (Plessix and Krupovnickas, 2021). Also, recent advancements in parallel computing, such as parallelizing workloads across multiple virtual or physical devices, have enabled FWI applications on a larger scale and/or to higher frequencies, with improved physical fidelity.

In this case study, we present results from a high-frequency elastic FWI model building workflow, using modern ocean bottom node (OBN) data acquired in 2021 over the Yggdrasil area, located in the Norwegian North Sea. Specifically, we focus on the imaging of the Frigg Gamma structure, above which distinct shallow geological features formed as the result of hydrocarbon leakage from the underlying reservoir (Rykkelid and Rundberg, 2014). This leakage is associated with significant calcite cementation, forming vertical pipe-like objects with extremely high interval velocities (exceeding 6000 m/s). These complex formations cause a seismically obscured area (SOA) underneath their location (Figure 1), making conventional seismic processing and imaging exceptionally difficult (Rykkelid et al., 2018; Raknes et al., 2018). Here, we show that high-frequency elastic FWI to 64 Hz, and its associated elastic FWI Image, help resolve the SOA to improve imaging of this key area.

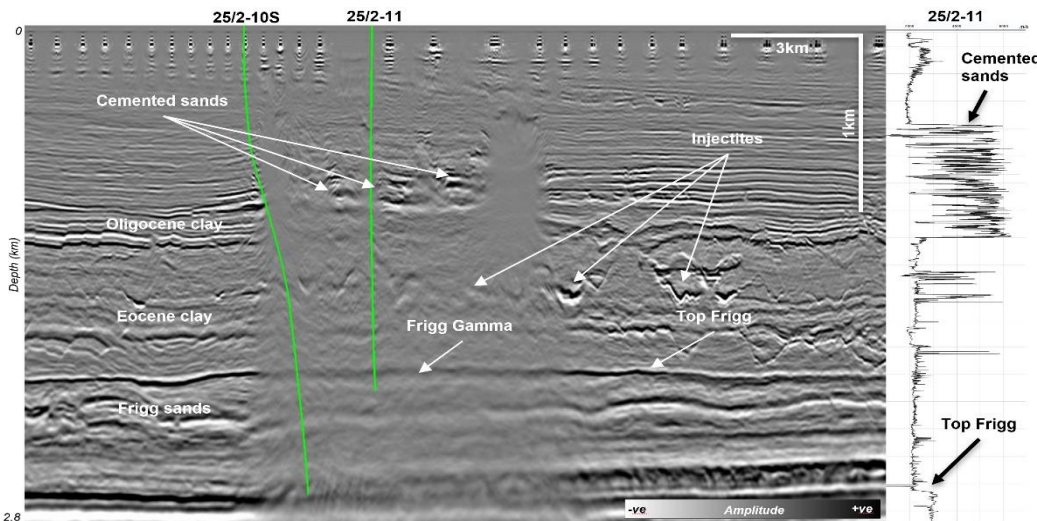


**Figure 1** Left: an arbitrary seismic line through two Frigg Gamma exploration wells. Right: a sonic log display of well 25/2-11 that was drilled through the seismically obscured area. The shallow part of the sonic log shows a massive increase in the compressional velocity caused by the cementation process.

### Data challenges and initial model generation

The OBN data set was acquired in a shallow-water marine environment (~120 m depth), with a strong water-bottom reflection coefficient (~0.4) leading to strong elastic effects associated with the hard water-sediment interface, such as guided waves, Scholte waves, etc. (Chen et al., 2024). In addition to the localized cementation above the Frigg Gamma structure, we also observe injectites and shallow gas accumulations typical in the Norwegian North Sea. Additionally, a strong velocity contrast associated with the Chalk Group (at approximately 2800 m deep) limits the diving-wave penetration in the offsets

used in this study. Further, we limit the analysis to a maximum depth of 2500 m; therefore, effects generated by the deeper geology were not considered. However, we note that it has been previously shown that elastic FWI can improve imaging of deeper targets in this area (Chen et al., 2024).

Prior imaging work here produced a tilted transverse isotropy velocity model using modern model building solutions, including 40 Hz acoustic Time-lag FWI (TLFWI; Zhang et al., 2018), combined with Q-FWI (Xiao et al., 2018) and multiple passes of travel-time tomography. After some small adjustments in the P-wave velocity (Vp) and anisotropy models, this was a good starting point for our work. A distinct regional velocity increase at Top Frigg was not fully captured by the previous velocity inversions. Using logs from multiple wells, correlated to the observed reflectivity, a multiple linear regression process was implemented to predict the velocity trend. Capturing the Top Frigg velocity increase in this model allowed it to be merged into the input model. The edited model was smoothed, to only leave the low-frequency background trend. Also, localized anomalies relating to sand injectite bodies were automatically interpreted on a reverse time migration (RTM) stack and used to generate a mask for anisotropy editing. The Vp/Vs ratio (Vs being the S-wave velocity) was estimated using shear and sonic logs from wells in the update area and was maintained during the FWI. Finally, density was computed from the velocity via an empirical power law,  $\rho = \alpha * V_p^\beta$ , where the coefficients  $\alpha$  and  $\beta$  were obtained from the available sonic and bulk density logs. Here, we derived spatially variable coefficients that provided a better match between the initial density model and the bulk density logs.

### Elastic FWI workflow and results

The OBN data used here has a shot depth of 7 m and an (x, y) spacing of 25 m by 50 m. Receivers were laid out on the seabed with 50 m by 300 m spacing in (x, y). The raw recorded data were deblended and standard OBN pre-processing was applied (tidal statics, source and receiver position correction, residual clock drift application and 3C rotation). Elastic FWI was run from 3 → 64 Hz and split into two key stages: the 1<sup>st</sup> stage utilized mainly transmitted arrivals, and the 2<sup>nd</sup> stage utilized the full wavefield. Both raw pressure and raw vertical geophone records were used to drive the inversion.

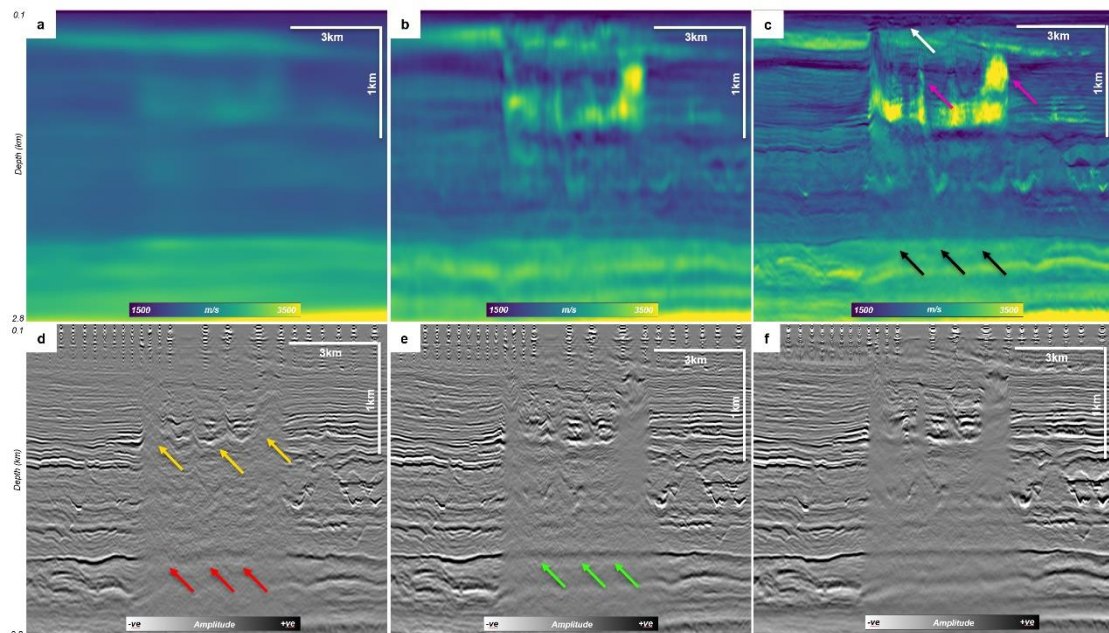


**Figure 2** Vp models and corresponding RTM images from: (a,d) starting model, (b,e) 1<sup>st</sup> stage elastic FWI update using transmitted energy, and (c,f) 2<sup>nd</sup> stage elastic FWI update using full wavefield.

Figure 2 shows the Vp models and corresponding RTM images at both stages of the update. The elastic FWI produces a high-resolution velocity model with a good level of detail, particularly in the area directly affected by the cementation (purple arrows on Figure 2c). Using the full wavefield, including multiples, the shallow section is also well resolved, with small gas accumulations being introduced as

visible low-velocity zones below the seabed (white arrow on Figure 2c). Despite the smooth initial model, elastic FWI was able to successfully resolve the geometry and small-scale features within the cementation zone and below. The velocity in the Frigg formation shows a continuous distribution, largely unaffected by the complex shallow structures (black arrows on Figure 2c).

Turning now to conventional imaging with these models, the RTM image when migrating data with the initial model shows significant undulations within the cemented pipes (yellow arrows on Figure 2d) and directly below. A lack of focusing on the Frigg Gamma structure with this initial model (red arrows on Figure 2d) may be expected given the complexity of the area. The 1<sup>st</sup> pass of FWI (Figure 2b) provides an RTM with better focusing and noise reduction, as noticeable at the Frigg Gamma structure, where the low-frequency Top Frigg reflection can be observed (green arrows on Figure 2e). After the 2<sup>nd</sup> stage FWI update, we see visibly reduced distortions of the shallow image in the cemented pipes area and further improvements in the image below (Figure 2f). However, as is clear from these images, despite the substantial increase in velocity model resolution, RTM using the primary-only upgoing wavefield is not able to fully illuminate the structures in the SOA, where significant dimming can still be observed, hindering interpretation of the Top Frigg and deeper events.

### FWI Imaging using elastic FWI

Despite the noticeable improvement in the RTM image migrated with the 64 Hz elastic FWI model, imaging beneath the cemented section still visibly suffers due to scattering and transmission losses in the recorded wavefield (Chen et al., 2024). The final 64 Hz elastic velocity model was used to produce an FWI Image (Zhang et al., 2020) and was compared with the RTM image using the same velocity model (Figure 3). By using the full wavefield, the FWI Image does a respectable job of resolving the amplitude dimming in the SOA observed in the RTM (Cooper and Ratcliffe, 2023), producing a more continuous amplitude distribution across the Top Frigg event and within the Frigg formation (green arrows on Figure 3b). The image at the shallower injectites interval (yellow arrow on Figure 3b) is also improved in the FWI Image, indicating structures that were not captured by the conventional RTM. Further, in the interval affected by the cementation, the FWI Image reveals structural complexity not previously seen in the area. Similar observations can be made in Figure 4, which contains constant depth slices at the injectite level (~1400 m). The RTM image (Figure 4a) shows the extent of the SOA (red dashed line) with visible amplitude dimming. The FWI Image of the same area (Figure 4b, green dashed line) produces an improved structural image that is much less affected by any amplitude loss.

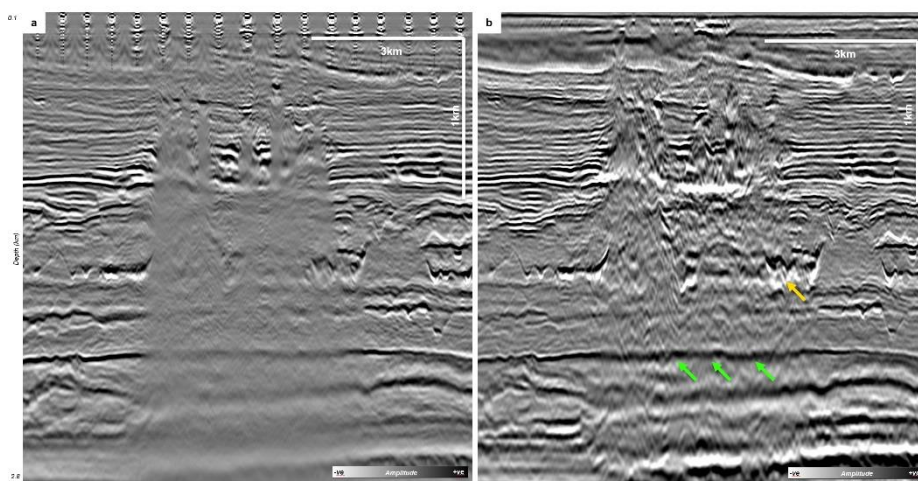


**Figure 3** (a) RTM image migrated with the 64 Hz elastic FWI model, and (b) FWI Image obtained from the 64 Hz elastic FWI velocity model.

### Conclusions

We presented an application of elastic FWI to 64 Hz on a shallow-water OBN data set from the Norwegian North Sea. We successfully recovered a high-resolution velocity model in an area that is

affected by a complex overburden consisting of shallow gas, cemented pipes and injectites. We have shown that the elastic FWI Image benefits from the full-wavefield illumination to produce a better image than RTM at the Frigg Gamma structure, which should lead to reduced interpretation uncertainty. This application of elastic FWI inverts for  $V_p$  only and relies on a good  $V_p/V_s$  model from well data, which might not always available. Hence, potential future work could involve updating  $V_s$  with elastic FWI using horizontal geophone data (Masmoudi et al., 2024).

### Acknowledgements

We thank Aker BP and their license partner on PL442 (ORLEN Upstream Norway) for permission to use the data and show the results, and Viridien for permission to publish.

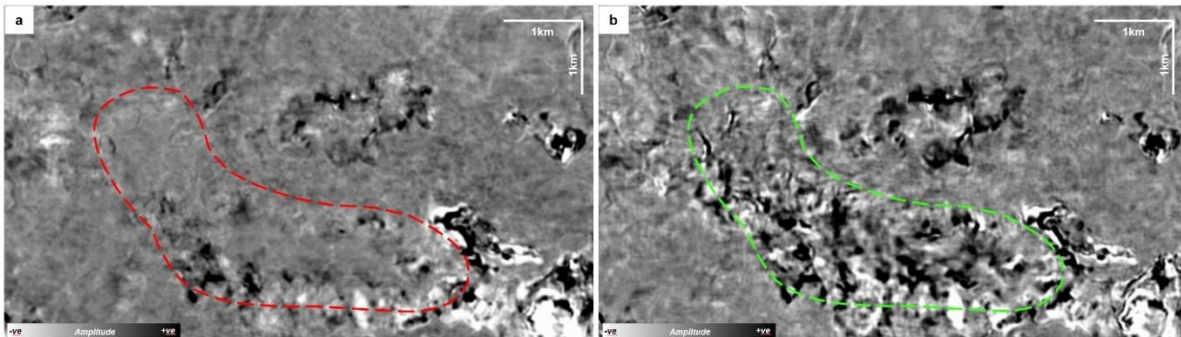


**Figure 4** Depth slices at 1400 m generated from: (a) RTM image migrated with the 64 Hz elastic FWI model, and (b) FWI Image obtained from the 64 Hz elastic FWI velocity model.

### References

Chen, X., Masmoudi, N., Ratcliffe, A., Mallows, M. and Tickle, J. [2024] Elastic Time-Lag full-waveform inversion using OBN data in shallow water environments. *85<sup>th</sup> EAGE Conference & Exhibition*, Extended Abstracts.

Cooper, J. and Ratcliffe, A. [2023] The role of FWI Imaging in Compensating for Transmission Loss. *84<sup>th</sup> EAGE Conference & Exhibition, Workshop Programme*, Extended Abstracts.

Masmoudi, N., Ratcliffe, A., Bukola, O., Tickle, J. and Chen, X. [2024] Elastic FWI of multi-component ocean-bottom seismic to update shear-wave velocity models. *85<sup>th</sup> EAGE Conference & Exhibition*, Extended Abstracts.

Plessix, R-E. and Krupovnickas, T. [2021] Low-frequency, long-offset elastic waveform inversion in the context of velocity model building. *The Leading Edge*, **40**(5), 342-347.

Raknes, E.B., Osen, A., Pettersen, R.S.H., Rykkelid, E. and Runde, Ø. [2018] Understanding the imaging challenges at the Frigg Gamma discovery. *80<sup>th</sup> EAGE Conference & Exhibition, Workshop Programme*, Extended Abstracts.

Rykkelid, E., Pettersen, E.H., Raknes, E.B., Runde, Ø., Denti, M., Hicks, E. and Vinje, V. [2018] Seismic processing challenges related to leakage of hydrocarbons from the Frigg Gamma field. *80<sup>th</sup> EAGE Conference & Exhibition, Workshop Programme*, Extended Abstracts.

Rykkelid, E. and Rundberg, Y. [2014] Seismic signature of hydrocarbon leakage from a Frigg Structure in the North Sea. *EAGE Shallow Anomalies Workshop, Indications of Prospective Petroleum Systems*, Extended Abstracts.

Xiao, B., Ratcliffe, A., Latter, T., Xie, Y. and Wang, M. [2018] Inverting for near-surface absorption with full-waveform inversion: a case study from the North Viking Graben in the northern North Sea. *80<sup>th</sup> EAGE Conference & Exhibition*, Extended Abstracts, Tu A12 03.

Zhang, Z., Mei, J., Lin, F., Huang, R. and Wang, P. [2018] Correcting for salt misinterpretation with full waveform inversion. *88<sup>th</sup> SEG Annual International Meeting*, Expanded Abstracts, 143-1147.

Zhang, Z., Wu, Z., Wei, Z., Mei, J., Huang, R. and Wang, P. [2020] FWI Imaging: Full-wavefield imaging through full-waveform inversion. *90<sup>th</sup> SEG Annual International Meeting*, Expanded Abstracts, 656-660.